Available online at www.sciencedirect.com
SCIENCE DIRECT®
International Journal of Solids and Structures 42 (2005) 2901–2910
INTERNATIONAL JOURNAL OF SOLIDS and STRUCTURES
www.elsevier.com/locate/ijsolstr

Size-scale effects on the friction coefficient

Alberto Carpinteri *, Marco Paggi

Politecnico di Torino, Department of Structural and Geotechnical Engineering, Corso Duca degli Abruzzi 24, 10129 Torino, Italy

Received 7 March 2004; received in revised form 2 October 2004
Available online 23 November 2004

Abstract

An overview of the classical friction laws holding at the macro-scale and the new developments at the nano-level are proposed. Furthermore, two opposite phenomena are addressed: the former concerning the apparent weakness of the San Andreas fault, the latter regarding the strong frictional behavior which appears at the nano-scale. An interpretation of these size effects on the friction coefficient is attempted making use of the renormalization group procedure which allows to explain the frictional phenomena over all the scales.

Keywords: Friction; Contact; Fractals; Geomechanics; Scale effects

1. Introduction

Friction is the resistance to motion that exists when a solid body is moved tangentially with respect to another, or when an attempt is made to produce such a motion.

Frictional phenomena are of great importance in everyday life and many processes are strongly dependent on the presence of friction. There are several classes of problems where a sufficiently large friction is desirable. For example, if the friction is too low, several simple processes such as cornering, braking and starting with a car will be difficult and dangerous. On the other hand, in many manufacturing processes where machinery parts are in relative motion, friction, and consequently wear, are undesirable effects and several efforts have been made to decrease the frictional resistance during sliding by lubrication and thorough shape design. A satisfactory understanding of this phenomenon at all size scales is one of the major research topics in physics.

* Corresponding author. Tel.: +39 011 564 4850/4910; fax: +39 011 564 4899.
E-mail address: alberto.carpinteri@polito.it (A. Carpinteri).

0020-7683/$ - see front matter © 2004 Elsevier Ltd. All rights reserved.
doi:10.1016/j.ijsolstr.2004.10.001

Then, since the phenomenological laws of friction were found by Amontons and Coulomb, a renewed interest to improve our understanding about the atomic level origins of friction, or nanotribology, has emerged in the last few years. This may partially stem from the need to miniaturize devices to nanometer scales and from the realization that friction laws on the nano-scale often differ from those on the macroscopic scale.

Nowadays, several theories confirmed by experimental studies have been set up by physicists and engineers at the opposite levels, the nano-scale and the macro-scale, although a unified friction theory over all the scales is still missing as well as several phenomena at opposite scales have not been explained yet with the current theory of friction.

Considering a type of friction largely governed by shearing of asperities and not by adhesive friction, the purpose of this paper is to review the main frictional theories holding at different scales, to show some inconsistencies and to interpret the frictional behavior over all the scales by a straightforward application of the Renormalization Group Theory.

2. Laws of sliding friction

Friction is expressed in quantitative terms as a force exerted by either of two contacting bodies tending to oppose relative tangential displacement of the other.

A first qualitative property of the friction force is the following: in any situation where the resultant of the tangential forces is smaller than some force parameter specific to that particular situation, the friction force will be equal and opposite to the resultant of the applied forces and no tangential motion will occur.

Otherwise, when the applied shear force, S, is sufficient to cause sliding, it is found experimentally that the body moves in the direction of S, and from this it follows that the friction force, although smaller than S, is still collinear with S. Then, it is possible to introduce a second qualitative property of the friction force: when tangential motion occurs, the friction force always acts in a direction opposite to that of the relative velocity of the surfaces.

The remaining laws of friction are concerned with the magnitude of the friction force. These classic friction laws were found by the French physicist Guillaume Amontons (first and second laws, 1699) and Charles-Augustin de Coulomb (third law, 1781), who described their observations of contacting solid surfaces as follows:

(1) friction is proportional to the applied normal force, $R \propto N$;
(2) friction is independent of the apparent or nominal contact area A_0;
(3) sliding friction is independent of the sliding velocity v for ordinary sliding velocities.

These laws apply surprisingly well on the macroscopic scale for dry friction (i.e. friction without lubrication).

Bowden and Tabor (1986) in 1950's found that, although friction is independent of the apparent contact area, it is proportional to the true contact area, that is $R \propto A_r$. Their discovery and their adhesion theory stem from the fact that real nominally flat surfaces are actually rough at the micro-scale. Thus, when two surfaces are pushed into contact one against the other, the contacting spots will be at the higher asperities of the surfaces, involving only a few percentage of nominal area into contact for the usual engineering range of applied loads.

Therefore, the real contact area will be the sum of any individual spot area, the normal load will be proportional to A_r and, for the first Amontons' law, the same proportionality will hold for the friction force.

About the friction dependence on the surface roughness, an increase has been found, over a wide range of surface roughness, in the friction coefficient with very smooth or very rough surfaces. In the former case,

the friction coefficient increases because the real area of contact grows excessively, whereas in the latter it is due to the need to lift one surface over the asperities of the other. In the intermediate range of roughness, friction is at a minimum and does not depend on the roughness (for more details, see Rabinowicz, 1995).

The check of the validity of these laws, that hold very well on the macroscopic scale, also on the atomic scale is an interesting research field. Recently, several authors, through experimental studies pursued with the atomic force microscope (Holscher and Schwarz, 2002), ultra-high vacuum conditions of a surface analysis apparatus (Schwarz et al., 1997a,b) and atomistic computer simulations (Wenning and Muser, 2001; Muser and Robbins, 2002), showed that the adhesive interaction between a nano-scale tip and a surface can be described by an Hertzian law modified to take into account the effect of adhesion. This means that the relationship between applied load and shear force for a single contact asperity is not linear as predicted by the Amontons' law and friction depends on the apparent area of contact.

Then, the recent investigations of frictional behavior at the nano-scale can be summarized into the following laws (Holscher and Schwarz, 2002):

(1) the energy dissipation takes place through stick-slip movements of individual atoms at the contact interface;
(2) atomic-scale friction depends on the size of the contact area, on the atomic structure and on the scan direction;
(3) friction is nearly independent of the sliding velocity.

The contradiction between the friction laws holding at the macro-level and those suggested at the nano-scale could be explained by the pioneering micromechanical contact models by Greenwood and Williamson (1966) and by Archard (1957). In fact, both assume an elastic Hertzian deformation model for each asperity in contact and show eventually a global linear relationship between normal load and real area of contact, in agreement with the Amontons' law.

Going into detail, the former suggests that the origin of the laws of friction, and particularly of the proportionality between area and load, lies not in the ideal plastic flow of individual contact spots but simply in the statistics of surface roughness where multi-asperity contact occurs. The latter, on the other hand, reaches the linear behavior through a deterministic hierarchical superposition of spheres of decreasing radius, with a surface model very similar to that of modern fractal theories.

3. Two opposite trends: the weakness of San Andreas fault and the strength at nano-scale interfaces

San Andreas fault (SAF) is one of the main components of the active transformation zones placed at the boundaries between North-American and Pacific plates. Very likely, it is the most studied fault all around the World.

For about 20 years, engineers and geophysicists have been very divided about the fundamental question on the magnitude of the shear stress resisting slip along the San Andreas fault, averaged over the upper 15 to 20 km of depth.

Several scientific programmes have been performed up to date, although the results often turned out to be inconsistent.

The problem to solve is the well-known heat-flow paradox: this consists in the fact that a straightforward application of the Byerlee's law (Byerlee, 1978; Detrick et al., 1986) to compute the average shear stress over the first 15 km of the fault plane depth, with an usual friction coefficient $f \cong 0.6$, typical of adjacent rocks, provides a value in contrast with the amount of heat-flow registered in shallow boreholes along the SAF. In fact, the value of $\overline{\tau} = 60\,\mathrm{MPa}$ predicted by the Byerlee's law would give rise to a thermal flux anomaly experimentally not checked (Lachenbruch and Sass, 1973, 1980).

Therefore, one should consider, consistently with the thermal relieves, that the shear level along the fault is less than 20 MPa. This value would suggest the fault to be weaker than the adjacent rocks where the Byerlee's law holds.

On the other hand, opposite reasoning about the supposed weakness of the fault arises from the friction coefficients $f = 0.6$ to 0.9 obtained by laboratory tests which are consistent with the Byerlee's range (Brace and Kohlstedt, 1980; Sibson, 1983). Such tests were performed on specimens extracted from the fault plane with hydrostatic pore pressure distribution.

Stress measurements performed in the Earth's crust at many sites around the World close to fault zones (McGarr and Gay, 1978; McGarr, 1980; Zoback and Healy, 1984; Townend and Zoback, 2000), indicate that the differential stress, $q = \sigma_1 - \sigma_3$, is high and approaches that predicted by Byerlee's law.

McGarr showed that an average shear tension level along the SAF, consistent with the thermal flux observed, can be typical only of weak rocks. Showing an increasing linear relationship between maximum shear stress, $t = (\sigma_1 - \sigma_3)/2$, and depth in good agreement with the experimental results, he expressed his doubts about the low value of the shear stress along the SAF, as previously assumed by Zoback and Healy (1984).

In support of this theory, as argued by Zoback and Healy (1984) and by Hickman (1991), the in situ measurements in several fault states show a fault intraplate strength in agreement with that predicted by the Byerlee's law, taking into account the hydrostatic pore pressure distribution. Moreover, Townend and Zoback (2000) detected by experimental techniques an high rock permeability which involves very likely an hydrostatic pore pressure distribution.

Recently, Scholz (2000) proposed a thesis of a strong San Andreas fault based on the friction coefficients included into the range 0.6–0.7, as observed in boreholes, assuming an hydrostatic pore pressure distribution. To explain the paradox, the author suggests that the heat-flow model is partially inconsistent, probably in the assumption that all heat transfer is governed by conduction.

In spite of many observations which suggest the evidence of strong intraplate faults such as a strong adjacent crust, several other experimental results give further evidence for a weak behavior.

In situ stresses along the San Andreas fault, determined from hydrofracture experiments, orientations of well-bore breakouts, geologic structure, and inversion of focal mechanism solutions from earthquake sources neighboring the fault zone, indicate that the maximum principal compressive stress is oriented at angles of 60°–80° from the plane of the fault, suggesting that the fault slips under low shear stress, consistently with the absence of the heat-flow anomaly (Zoback et al., 1987; Oppenheimer et al., 1988; Wong, 1990).

Furthermore, measurements of stress heat flow to depths of 3.5 km in the Cajon Pass borehole indicate high differential stress level adjacent to the San Andreas (i.e. a strong crust), although the San Andreas fault itself is relatively weak (Lachenbruch and Sass, 1992; Zoback and Healy, 1992; Lachenbruch et al., 1995).

Recently, analysis of stress-induced borehole breakouts in petroleum wells along the SAF indicate that the angle between the maximum horizontal compressive stress and the San Andreas fault increases from 25° to 45° near the fault to 65° to 85° at distances greater than 20 km (Castillo and Hickman, 1995), suggesting that in this segment the SAF is able to support higher levels of shear stress as compared to other weaker segments of the fault.

According to such experimental analyses, assuming a coefficient of friction, f, equal to 0.6–0.9 on the SAF, as predicted by Byerlee's law, the heat-flow constraint would be satisfied only if the in situ pore pressure, σ_w, is greater than twice the hydrostatic one (Lachenbruch and Sass, 1980, 1992). To explain this theory, we can observe that high water pressure affects the Mohr's circles moving the origin of the Mohr–Coulomb failure envelop toward higher values of σ_n. Then, for the same minimum principal stress, the tangential stress acting on the plane of maximum obliquity will be less than the value corresponding to an hydrostatic pressure distribution.

However, if one assumes that principal stress magnitudes are constant across the fault zone and that $f \geqslant 0.6$, then high fluid pressures alone cannot explain the directional constraint as σ_w would exceed the

least principal stress once the angle between $\sigma_{h,\max}$ and the fault plane exceeds about 60° (Zoback et al., 1987; Scholz, 1989; Lachenbruch and McGarr, 1990).

It has recently been suggested that large-scale yielding could lead to an increase in the magnitudes of the principal stresses within the fault zone with respect to their values immediately outside of the fault (Rice, 1992) (see Fig. 1).

Therefore, Rice (1992) suggests that an inhomogeneous stress distribution and fluid pressure distribution could allow slip on the SAF under the prevailing in situ stress, although the fault has a normal friction coefficient (i.e. a strong fault). The high pore pressure could be maintained either by upflow of fluids from depth along a relatively permeable fault zone (Rice, 1991), or by trapping fluids at high pressure in an effectively low permeable zone (Byerlee, 1990).

On the other hand, always assuming an inhomogeneous stress distribution, the phenomenon can also be explained supposing an homogeneous hydrostatic pore pressure and a low friction coefficient (i.e. a weak fault) (Lachenbruch and McGarr, 1990; Lachenbruch and Sass, 1992) (see Fig. 2).

It is often proposed that the presence of clays or other weak minerals along the SAF might lead to an anomalous low frictional resistance (Chester et al., 1993). The same authors, by the analysis performed on exhumed faults of the SAF system (San Gabriel fault and Punchbowl fault), pointed out an internal structure which could allow high pore pressure distributions. Likely, several mechanisms operate in conjunction to produce the weak behavior of the SAF and of the major faults, such as dynamic weakening mechanisms, frictional melting and lubrication, thermal pressurization of pore fluids.

As the San Andreas fault shows a weak behavior at large scale, at the opposite scale, that is the nano-level, a strong behavior appears when friction is governed by shearing of asperities, not by adhesive friction. At the nano-scale, in fact, it is also possible to have very small values of the friction coefficient associated with Van der Waals forces. However, if single asperity contact breakdown involves shearing of small volumes, then the theoretical strength (or approaching it) may be invoked.

Gerberich et al. (2002) consider how the local dislocation arrangement below a single point contact might affect the local stress and therefore the failure criterion for the initial stage of light wear as indicated by an observed large change in the friction coefficient. The authors, considering the amount of pile-up in a material that occurs around plastically deforming contacts, represent the number of dislocations released from a pile-up when an oxide film breaks down. Based on a continuum approach, they found

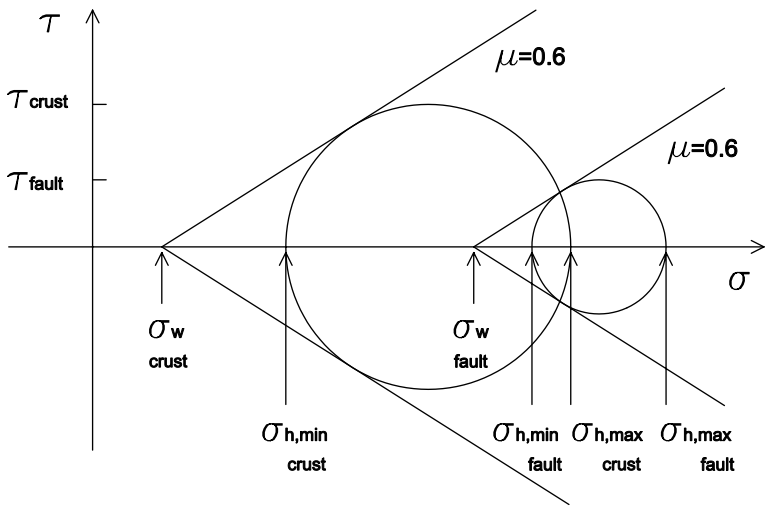

Fig. 1. Strong fault: the pore pressure is hydrostatic outside the fault zone, but is about lithostatic inside.

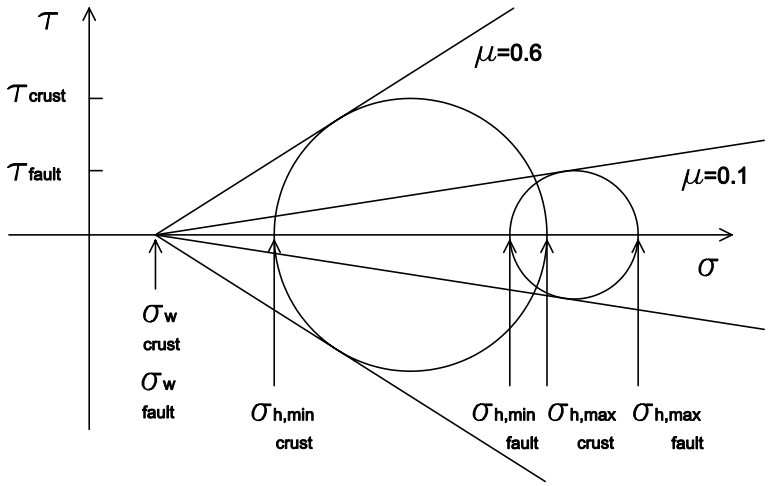

Fig. 2. Weak fault: the pore pressure is hydrostatic everywhere but the friction coefficient is low inside the fault zone.

the relationship among this critical number, n_{cr}, the information on how robust the oxide film is and the relevant severity of the dislocation pile-up, by introducing a volume to surface ratio representing the plastic zone volume around a contact and the projected area of the contact itself.

Moreover, they considered two sets of experiments involving tungsten and tantalum single crystals. The former set was designed to evaluate whether or not an oxide layer breaks at the displacement excursion δ resulting in a release of piled-up dislocations as expected by the theoretical value of n_{cr}. The latter was performed to compare normal force and lateral force induced by fretting fatigue.

The results, consistent with the predicted theoretical values, demonstrate plastic deformation at lower loads even in absence of a yield point. When oxide break down occurs, a jump in normal displacement leads to a huge increase in lateral force and the friction coefficient rises from 0.2 to 4.8.

During this phenomenon it is hypothesized that the dislocations are gradually piling up at the oxide interface and when there are enough of them sufficiently accumulated, oxide break down occurs. The normal displacement evolution during these lateral tests of fretting fatigue is not accumulating linearly cycle by cycle and a large yield excursion has been observed.

4. Scale-independent interpretation by renormalization group theory

As above addressed, a unified friction theory which holds over all the scales is still missing. Weak and strong behavior respectively at very large and very small scales suggest that friction is scale-dependent and that the theories which describe quite well the phenomenon at one scale, fail when applied at other scales.

Considering friction largely governed by shearing of asperities, a straightforward interpretation by Renormalization Group procedure (Wilson, 1971) could be able to furnish a scale-independent law.

As previously proposed for the size-scale effects on tensile strength and fracture toughness (Carpinteri, 1994a,b), it is impossible to measure these constant properties unless we depart from the integer dimensions of the material ligament at the peak load and of the fracture surface at the final rupture. Only in this way it is possible to define new mechanical properties which turn out to be scale-invariant material constants.

Borri-Brunetto et al. (1999) found, by means of extensive numerical experiments, the fractality of the contact domain between elastic bodies with random rough boundaries. It can be realized that the concept of true contact area is not able to describe consistently (that is, in a scale-independent manner) the contact

problem, because, increasing the resolution, the contact area progressively decreases tending to zero in the theoretical limit of infinite resolution, while the local pressure tends to infinity.

In perfect analogy with the theory of fractal scaling applied to nominal tensile strength, Borri-Brunetto et al. considered the following Renormalization Group:

$$N = \sigma_0 A_0 = \sigma_1 A_1 = \cdots = \sigma_i A_i = \cdots = \sigma^* \mathscr{H}_{D_\sigma}, \tag{1}$$

where N is the applied normal load (scale-invariant quantity), A_i and σ_i are respectively the nominal contact area ($[L]^2$) and the nominal mean pressure ($[F][L]^{-2}$) measured at the i-th prefractal scale. In the theoretical limit of the highest resolution, the Euclidean description loses its significance and leaves place to the Hausdorff measure $\mathscr{H}_{D_\sigma}$ of the contact domain, D_σ, (defined by the noninteger dimension $[L]^{\Delta_\sigma}$, where Δ_σ is the Hausdorff dimension of the contact domain). The fractal mean pressure, σ^*, defined by the anomalous physical dimensions $[F][L]^{-\Delta_\sigma}$ results to be scale-independent. Moreover, it is possible to obtain a scaling law which states the dependence of the nominal pressure, $\sigma_0 = N/A_0$, on the characteristic linear size of the specimen, b. By equating the second and the last term in Eq. (1) and taking the logarithm of both sides, we obtain:

$$\ln(\sigma_0 A_0) = \ln(\sigma^* \mathscr{H}_{D_\sigma}), \tag{2}$$

$$\ln(\sigma_0 b^2) = \ln(\sigma^* b^{\Delta_\sigma}). \tag{3}$$

Equation (3) can be rearranged and the following scaling law can be provided:

$$\ln \sigma_0 = \ln \sigma^* - (2 - \Delta_\sigma) \ln b. \tag{4}$$

A similar scaling law can be written for friction resistance considering the following Renormalization Group:

$$S = \tau_0 A_0 = \tau_1 A_1 = \cdots = \tau_i A_i = \cdots = \tau^* \mathscr{H}_{D_\tau}, \tag{5}$$

where S is the applied shear load (scale-invariant quantity), which is equilibrated by the friction resistance, R. In the theoretical limit of the highest resolution, the Hausdorff measure $\mathscr{H}_{D_\tau}$ of the contact domain, D_τ, where the effective shear strength is activated, defined by the noninteger dimension $[L]^{\Delta_\tau}$, holds. By equating the second and the last term in Eq. (5) and taking the logarithm of both sides, we obtain:

$$\ln(\tau_0 A_0) = \ln(\tau^* \mathscr{H}_{D_\tau}), \tag{6}$$

$$\ln(\tau_0 b^2) = \ln(\tau^* b^{\Delta_\tau}). \tag{7}$$

Equation (7) can be rearranged and the following scaling law can be provided:

$$\ln \tau_0 = \ln \tau^* - (2 - \Delta_\tau) \ln b. \tag{8}$$

The fractal friction coefficient, f^*, takes into account the dimensional disparity between normal and tangential stresses and represents the scale-invariant property of the interface. According to Chiaia (2002), a fractal Coulomb law can be then postulated to link these fractal quantities:

$$\tau^* = f^* \sigma^*. \tag{9}$$

In particular, at each scale the Coulomb law can be written as follows:

$$\ln f = \ln\left(\frac{\tau_0}{\sigma_0}\right) = \ln \tau_0 - \ln \sigma_0, \tag{10}$$

$$\ln f^* = \ln\left(\frac{\tau^*}{\sigma^*}\right) = \ln \tau^* - \ln \sigma^*. \tag{11}$$

By substituting Eqs. (4) and (8) into Eq. (10), we obtain the following relationship:

$$\ln f = \ln \tau^* - (2 - \Delta_\tau) \ln b - \ln \sigma^* + (2 - \Delta_\sigma) \ln b. \tag{12}$$

Finally, substituting Eq. (11) into Eq. (12), a scaling law which states the dependence of the apparent friction coefficient on the size of the specimen, b, is provided:

$$\ln f = \ln f^* - (\Delta_\sigma - \Delta_\tau) \ln b, \tag{13}$$

where the difference $(\Delta_\sigma - \Delta_\tau)$ is always positive according to the results obtained by Borri-Brunetto et al. (2001) and by Chiaia (2002). Going into the details, the authors generated fractal surfaces characterized by several fractal dimensions and resolutions by applying the random midpoint displacement method. Afterwards, a direct treatment of the fractal normal and tangential contact problem, fully taking into account elastic deformations of the half-spaces, was proposed. Their numerical results proved the scaling law for the nominal mean pressure given by Eq. (4), and, by using the box counting method, observed that the critical shear strength is activated within a subset of the contact domain whose dimension Δ_τ is lower than Δ_σ.

In 1993 Wang and Scholz (1993) set up a contact model based on the Cattaneo–Mindlin's technique to study the frictional behavior of rock joints treated as rough surfaces in contact under normal and shear loads. In particular, the authors generated fractal surfaces whose asperities were assumed to have a spherical shape. The tangential displacement of each asperity was modeled according to the following relationship:

$$\delta_i = \frac{3fN_i}{16a}\left(\frac{2-\nu_1}{G_1} + \frac{2-\nu_2}{G_2}\right)\left[1 - \left(1 - \frac{S_i}{fN_i}\right)^{2/3}\right], \tag{14}$$

where G and ν are the shear modulus and the Poisson's ratio, and the subscripts 1 and 2 indicate bodies 1 and 2, respectively. S_i and N_i are the normal and the shear loads acting at each asperity, and a is the contact radius.

The authors found a power law relationship between the critical slip distance, D, which is the distance at which the majority of contacts have changed from partial sliding to full sliding condition, and the correlation length of the surfaces.

Furthermore, they showed that the frictional behavior is mainly determined by the surface roughness with the wavelengths greater than the correlation length, i.e. the uncorrelated part of the roughness.

They also proved that the critical slip distance increases with the increase in the correlation length, assuming a constant coefficient of friction in all the numerical simulations. On the basis of this result provided by Wang e Scholz, we may interpret this phenomenon as a size-scale effect on the friction coefficient. In fact, according to the Cattaneo–Mindlin's solution, each asperity slips when $S_i = fN_i$ and the corresponding slip displacement is given by

$$\delta_i = \frac{3fN_i}{16a}\left(\frac{2-\nu_1}{G_1} + \frac{2-\nu_2}{G_2}\right). \tag{15}$$

Therefore, the authors, by assuming a constant friction coefficient in their simulations, observed an increase in the critical tangential displacement of each asperity given by Eq. (15) and a corresponding increase in the critical slip distance. On the other hand, if we permit the friction coefficient to vary in order to have a constant critical slip distance during the contact simulations, the friction coefficient should decrease as the correlation length increases, according to our scaling law.

Equation (13) has been depicted for $(\Delta_\sigma - \Delta_\tau) = 0.15$ in Fig. 3. Point A ($b = 100$ nm, $f = 4.6$) may be representative of the results obtained on the nano-level, point B ($b = 10$ cm, $f = 0.6$) may be representative of the laboratory friction tests upon SAF specimens and point C ($b = 100$ m, $f = 0.2$) may characterize the weak behavior of the fault. The value of the parameter b for the last point is in agreement with the expected

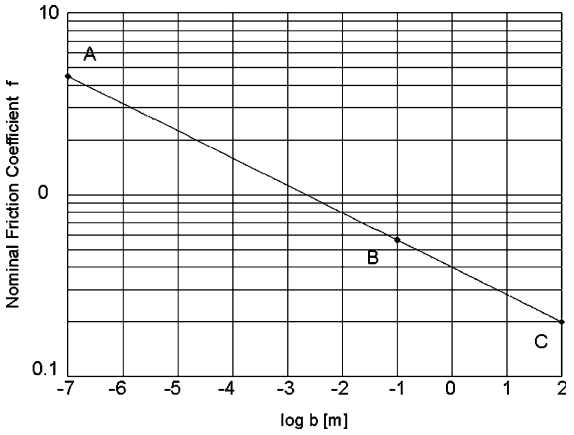

Fig. 3. Size-scale effect on the nominal friction coefficient f.

range of correlation length predicted by Wang and Scholz for large faults, which appears to be from few tens to few hundreds meters.

In conclusion, the law of Eq. (13) is able to explain the scale effects previously observed: at large scales (i.e. large b like it happens for the SAF) the coefficient of friction decreases giving rise to a weak behavior, whilst at small scales (i.e. small b like it happens at the nano-level) the behavior is much stronger.

Acknowledgement

Support by the Italian Ministry of University and Scientific Research (MIUR) is gratefully acknowledged.

References

Archard, J., 1957. Elastic deformation and the laws of friction. Proceedings of the Royal Society of London Ser. A 243, 190–205.

Borri-Brunetto, M., Carpinteri, A., Chiaia, B., 1999. Scaling phenomena due to fractal contact in concrete and rock fractures. International Journal of Fracture 95, 221–238.

Borri-Brunetto, M., Chiaia, B., Ciavarella, M., 2001. Incipient sliding of rough surfaces in contact: a multiscale numerical analysis. Computational Methods in Applied Mechanics and Engineering 190, 6053–6073.

Bowden, F., Tabor, D., 1986. The Friction and Lubrication of Solids. Clarendon Press, Oxford.

Brace, W., Kohlstedt, D., 1980. Limits on lithospheric stress imposed by laboratory experiments. Journal of Geophysical Research 85, 6248–6252.

Byerlee, J., 1978. Friction of rocks. Pure and Applied Geophysics 116, 615–629.

Byerlee, J., 1990. Friction, overpressure and fault normal compression. Geophysical Research Letters 17, 2109–2112.

Carpinteri, A., 1994a. Fractal nature of material microstructure and size effects on apparent mechanical properties. Mechanics of Materials 18, 89–101.

Carpinteri, A., 1994b. Scaling laws and renormalization groups for strength and toughness of disordered materials. International Journal of Solids and Structures 31, 291–302.

Castillo, D., Hickman, S., 1995. Near-field stress and pore pressure observations along the Carrizo Plain segment of the San Andreas fault. Eos, Transactions of AGU, F558 76, 2005–2012.

Chester, F., Evans, J., Biegel, R., 1993. Internal structure and weakening mechanisms of the San Andreas fault. Journal of Geophysical Research 98, 771–786.

Chiaia, B., 2002. On the sliding instabilities at rough surfaces. Journal of the Mechanics and Physics of Solids 50, 895–924.

Detrick, R., von Herzen, R., Parsons, B., Sandwell, D., Dougherty, M., 1986. Heat flow observations on the Bermuda Rise and Thermal Models of Mid-Plate Swells. Journal of Geophysical Research 91, 3701–3723.

Gerberich, W., Tymiak, N., Kramer, D., Daugela, A., 2002. An approach to dry friction and wear for small volumes. Philosophical Magazine A: Physics of Condensed Matter, Structure, Defects and Mechanical Properties 82, 3349–3360.

Greenwood, J., Williamson, J., 1966. Contact of nominally flat surfaces. Proceedings of the Royal Society of London Ser. A 295, 300–319.

Hickman, S., 1991. Stress in the lithosphere and the strength of active faults. Review of Geophysics 29, 759–775.

Holscher, H., Schwarz, U., 2002. Friction at the nanometer-scale—nanotribology studied with the atomic force microscope. Publications of Scanning Probe Methods Group, 2002.

Lachenbruch, A., McGarr, A., 1990. Stress and heat flow, in the San Andreas Fault System, California. US Geol. Surv. Prof. Paper 1515, pp. 261–277.

Lachenbruch, A., Sass, J., 1973. Thermo-mechanical aspects of the San Andreas fault system. In: Proceedings of the Conference on Tectonic Problems of the San Andreas Fault System. pp. 192–205.

Lachenbruch, A., Sass, J., 1980. Heat flow and energetics of the San Andreas fault zone. Journal of Geophysical Research 85, 6185–6223.

Lachenbruch, A., Sass, J., 1992. Heat flow from Cajon Pass, fault strength and tectonic implications. Journal of Geophysical Research 97, 4995–5015.

Lachenbruch, A., Sass, J., Clow, G., Weldon, R., 1995. Heat flow at Cajon Pass, California, revisited. Journal of Geophysical Research 100, 2005–2012.

McGarr, A., 1980. Some constraints on levels of shear stress in the crust from observations and theory. Journal of Geophysical Research 85, 6231–6238.

McGarr, A., Gay, N., 1978. State of stress in the Earth's crust. Annual Review of Earth and Planetary Sciences 6, 405–436.

Muser, M., Robbins, M., 2002. Atomistic computer simulations of friction between solids. SIMU Challenges in Molecular Simulations 4, 101–117.

Oppenheimer, D., Reasenberg, P., Simpson, R., 1988. Fault-plane solutions for the 1984 Morgan Hill, California earthquake sequence: Evidence for the state of stress on the Calaveras fault. Journal of Geophysical Research 93, 9007–9026.

Rabinowicz, E., 1995. Friction and Wear of Materials. John Wiley & Sons, Inc., New York, NY.

Rice, J., 1991. Friction, pore pressure, and the apparent weakness of major faults. Available from: <http://www.geophysics.rice.edu/margins/workshop.reports/rice/Rice.html>.

Rice, J., 1992. Fault stress states, pore pressure distributions, and the weakness of the San Andreas fault. In: Evans, B., Wong, T.-F. (Eds.), Fault Mechanics and Transport Properties of Rocks. Academic Press, New York, pp. 475–503.

Scholz, C., 1989. Mechanics of faulting. Annual Review of Earth and Planetary Sciences 17, 309–334.

Scholz, C., 2000. Evidence for a strong San Andreas fault. Geology 28 (2), 163–166.

Schwarz, U., Zwörner, O., Köster, P., Wiesendanger, R., 1997a. Quantitative analysis of the frictional properties of solid materials at low loads. i. Carbon compounds. Physical Review B 56, 6987–6996.

Schwarz, U., Zwörner, O., Köster, P., Wiesendanger, R., 1997b. Quantitative analysis of the frictional properties of solid materials at low loads. ii. Mica and germanium sulfide. Physical Review B 56, 6997–7000.

Sibson, R., 1983. Continental fault structure and the shallow earthquake source. Journal of the Geological Society of London 140, 741–767.

Townend, J., Zoback, M., 2000. How faulting keeps the crust strong. Geology 58 (6), 399–402.

Wang, W., Scholz, C., 1993. Scaling of constitutive parameters of friction for fractal surfaces. International Journal of Rock Mechanics 30, 1359–1365.

Wenning, L., Muser, M., 2001. Friction laws for elastic nanoscale contacts. Europhysical Letters 54 (5), 693–699.

Wilson, K., 1971. Renormalization group and critical phenomena. Physical Review B 4, 3174–3205.

Wong, I., 1990. Seismotectonics of the coast ranges in the vicinity of Lake Berryessa, Northern California. Bulletin of the Seismological Society of America 80, 935–950.

Zoback, M., Healy, J., 1984. Friction, faulting, and in situ stresses. Annales Geophysicae 2, 689–698.

Zoback, M., Healy, J., 1992. In situ stress measurements to 3.5 km depth in the Cajon Pass scientific research borehole: Implications for the mechanics of crustal faulting. Journal of Geophysical Research 97, 5039–5057.

Zoback, M., Zoback, M., Mount, V., Suppe, J., Eaton, J., Healy, J., Oppenheimer, D., Reasenberg, P., Jones, L., Raleigh, C., Wong, O., Scotti, O., Wentworth, C., 1987. New evidence on the state of stress of the San Andreas fault system. Science 238, 1105–1111.